Grains, Growth, and Grooving

M. J. Rost, D. A. Quist, and J. W. M. Frenken
Kamerlingh Onnes Laboratory, Leiden University, P.O. Box 9504, 2300 RA Leiden, The Netherlands
(Received 7 November 2002; published 7 July 2003)

We report the *in situ* investigation of grain growth and grain boundary migration, performed with a variable-temperature scanning tunneling microscope (STM) on a polycrystalline gold film. Atomic step resolution allowed us to identify the individual grains and, thus, also the grain boundaries. Our special, thermal-drift-compensated STM design made it possible to follow the same sample area over large temperature intervals. In this way, we have directly observed grain boundary migration and grain growth. In a first quantitative analysis we correlate the observed, unexpected changes in surface roughness with the evolution of the grain and grain boundary configuration.

DOI: 10.1103/PhysRevLett.91.026101 PACS numbers: 68.55.–a, 61.72.Mm, 68.35.Ct, 68.37.Ef

Metals and most other solid materials appear most commonly in polycrystalline form, which means that they consist of many small, single-crystalline grains. Since many properties, e.g., mechanical, electronic, magnetic, optical, or chemical, are influenced and often even dominated by the specific grain structure, this grainy structure is manipulated in process technology, e.g., by heat and stress treatments. In thin film technology, next to the grain structure, the surface roughness forms an important structural parameter. As will be shown, grain structure and surface roughness are related to one another via the condition that the surface is in equilibrium at all triple lines [1], where grain boundaries (GBs) intersect the surface. In turn, surface roughness is known to influence the migration of grain boundaries [2]. Since the decay rate of surface roughness depends on the surface-atom mobility, the specific surface transport kinetics could also affect the grain growth kinetics.

In situ bulk observation of the evolution (grain growth) of polycrystalline metals, especially during heat treatment, proves to be difficult [3,4]. Recent developments in x-ray tomography have enabled the determination of accurate 3D images of polycrystalline Al [5]; however, the GBs had to be decorated with Sn. The first progress in the observation of single-material dislocations has been reported very recently by Larson *et al.* [6]. In some special cases the migration study of a single, artificially created GB is possible [7–9] by using diffraction contrast in scanning electron microscopy. It is possible to study grain growth during heat treatment in very thin films by using transmission electron microscopy (TEM) [10]. However, when the film thickness is in the order of the individual grain size, grain growth [11] and other evolution effects depend on surface morphology, as suggested by Dannenberg *et al.* [12]. In these cases the TEM observation is incomplete, because of the lack of surface information [12]. Reviews of experimental and theoretical grain growth work can be found in [13,14,15].

Here we describe the direct observation of GB motion and grain growth with an ultrahigh vacuum (UHV) STM. Atomic step resolution on all grains allows us to correlate changes in the surface roughness with changes in the film structure. We have investigated the structure of polycrystalline gold films and followed their evolution during *in situ* heat treatments on a sufficiently small scale to distinguish the mechanisms at work. We observe a strong initial decrease in film roughness, followed by a slow increase at later stages. This roughness evolution is accompanied by changes in both the grain orientations and the average grain size. We find that precisely these changes are responsible for the roughness evolution.

The gold films were prepared *in situ,* in order to avoid contamination. As a substrate we used polished quartz, $SiO_2(0001)$, which we measured to be atomically flat over hundreds of nm [16]. The 30 nm thick films were deposited at pressures lower than 10^{-9} mbar from a well-outgassed Knudsen cell with 99.999% pure gold at a low rate of $\sim$1 nm/h, with the substrate remaining at room temperature. Immediately after deposition, the samples were transferred to the STM without breaking UHV. Our home-built, thermal-drift-compensated STM [17] allowed us to vary the sample temperature over more than 250 K while observing the same sample area. All STM images were acquired at a sample voltage of -0.7 V and at tunneling currents below 0.1 nA.

Figure 1 shows a 33 nm thick film, directly after deposition at room temperature: each protrusion is an individual grain with a different orientation, as can be verified from the heights and shapes of the atomic steps visible on the grains. X-ray diffraction measurements perpendicular to the substrate ($\theta/2\theta$ scans) on similarly prepared samples show a [111] texture ($\sim 84\%$) with $\sim$16% [100] grains and no [110] grains (weighted with respect to gold powder diffraction intensities). The range of grain misorientation is reflected in the rocking curve width of the [111] peak: 2.8°. Using such samples as the starting configuration, we recorded STM movies of the film evolution during a heat treatment. While we increased the temperature over a period of 24 h from 293 to 748 K, we continually monitored the film with the

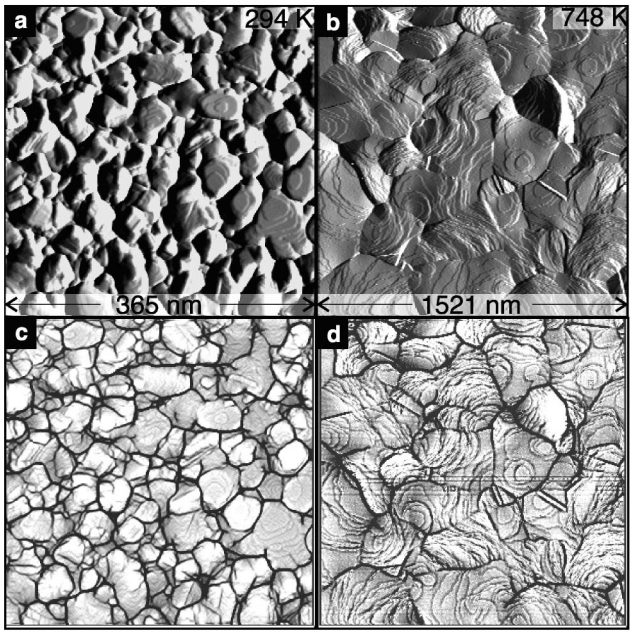

FIG. 1. STM images (a),(c) immediately after deposition at 293 K and (b),(d) at 748 K. Notice the larger scale in panels (b),(d). We used a differential filter for (a) and (b) in order to obtain a high step contrast, and a special filter for (c) and (d) in order to enhance the contrast on the grain boundaries.

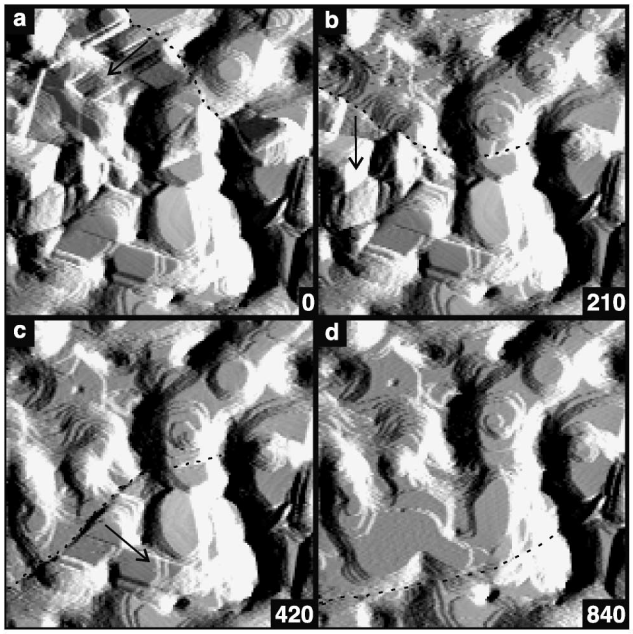

FIG. 2. Four images (172 nm) selected from an STM movie illustrate GB migration at 413 K. The time (sec) is indicated in the images. Notice the flatter, more (111) oriented region, which is left behind by the moving GB.

STM. In our STM movies [18] we followed individual surface regions during temperature changes up to 75 K. Figure 1(b) illustrates the final result of the annealing experiment (notice the larger length scale). The average grain size has increased by an order of magnitude, the film roughness has decreased, and more grains are oriented with their [111] axis perpendicular to the substrate (texture): almost exclusively (111) terraces are visible. X-ray measurements also reveal an enhancement in [111] texture, since the peak area has increased by a factor of 6.4. In addition, we see the complete disappearance of the [100] signal. Texturing can occur during deposition as well as post-deposition annealing [19]. Driving forces for the reconfiguration of the grain structure stem from the texture dependent intrinsic stress [20] and from the free energies of both the film-surface and the film-substrate interface [14].

Our movies [18] show two different evolution mechanisms. Usually, grains grow continuously at the expense of their neighbors (*normal grain growth*). In a small number of cases, at temperatures below 468 K, we have seen a GB sweeping through the film; Fig. 2 illustrates such an observation in four images from the second movie of [18], taken at 413 K. The position of the GB, which can be easily identified by comparing consecutive images in the movie, is indicated with a thin, dotted line. It sweeps through the imaged area within 15 min (~ 2 Å/s). While the small grains in front of the GB show a wide variety in orientations, as can be judged from the differences in slopes (gray levels) and symmetries (rectangular, hexagonal, etc.), the region left behind by the passing GB is much flatter and contains only four grains, each with a prominent [111] texture. Sweeping reorientation fronts are well known in metallurgy [13], e.g., in materials with *abnormal grain growth* or in crystals that are highly deformed via cold rolling. However, we relate our observation to *orientation pinning,* where GBs evolve into low-angle configurations with low mobility. The high-angle grain boundaries have a much higher mobility and sweep through the film until also they are trapped into a low-energy configuration. This is what we observe with the GB of Fig. 2, which gets stuck at the position of Fig. 2(d) for the remaining $\sim$120 min of the movie.

It is possible, in principle, to identify the bulk crystallographic orientations of all grains by using a combination of the observed step-height and step-orientation information on individual grains together with the grain shapes. Here we have restricted our analysis to the evolution of the average grain size and the roughness of the film. The average grain size can be determined relatively easily from the number of grains counted by eye in the STM images. The reliable determination of the film roughness requires a more sophisticated approach. We define the roughness of the film R as the asymptotic value of the root mean square (rms) height variation of the film, for long distances with respect to the average grain size. From each STM image, the rms height variation was measured as a function of the length scale L (size of sampling area). As an illustration, in Fig. 3(a), $R = 0.93$ nm is reached for $L = 280$ nm, which is slightly more than 2 times the average grain size of 115 nm measured at this stage of the film evolution.

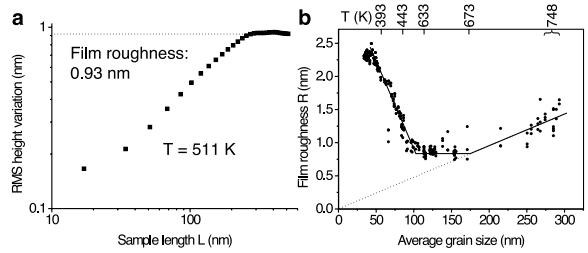

FIG. 3. (a) The graph of the rms height variation as a function of the length scale L levels off at $\sim$0.93 nm. This value represents the roughness R of the film at this stage. (b) Film roughness R as a function of the average grain size. Each individual point has been determined with the procedure illustrated in (a). Notice that the roughness first decreases, then stays almost constant, and later increases again.

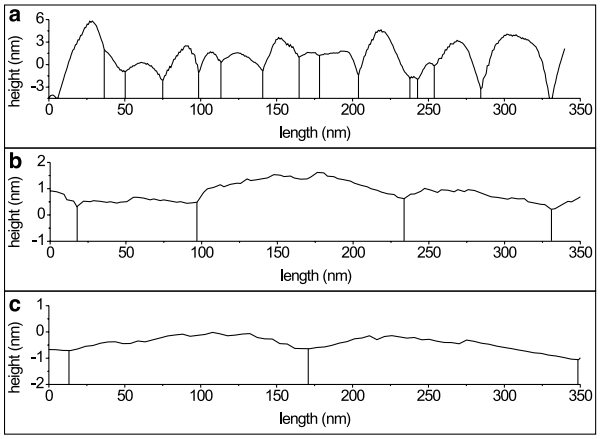

FIG. 4. Typical STM height lines of the Au film (a) immediately after deposition, (b) at 668 K, and (c) at 748 K. Each dome is an individual grain. Vertical lines indicate the grain boundary locations. Note the different height scales. In panels (b),(c) individual steps and terraces are visible.

Figure 3(b) shows the film roughness R as a function of the average grain size, e.g., as a function of the stage of film evolution. The upper horizontal axis denotes the corresponding temperatures. To our surprise, the roughness initially drops by a factor of 3, remains constant over a few hundred K, and increases again at the highest temperatures; such behavior has been noticed before in *ex situ* experiments by Porath *et al.* [21], who suggested that it could be due to a competition between GB mobility and surface diffusion. As we argue in the following, our observations show that GB motion is already quite active at low temperatures, and surface diffusion has no problem making the surface morphology adapt to the moving GBs at high temperatures. In fact, the activation energy for GB motion in gold can be as low as 0.14 eV [22], while that for mass transport on gold surfaces is on average 0.9 eV [23]. Our *in situ* film observations reveal that over the entire temperature interval, from room temperature up to 748 K, GB motion and surface morphology changes always occurred simultaneously.

Figure 4 shows typical scan lines at three stages of the film evolution. Each grain shows a dome-shaped top without any positively curved part. Careful inspection of the atomic steps shows that each dome corresponds to one single grain. As we will explain now, each configuration of Fig. 4 represents the equilibrium surface profile at that stage of the film's evolution.

Equilibrium between the three interfaces that meet at the triple line, where a GB intersects the surface, requires a set of angles, α_{GB}, α_{S1}, and α_{S2}, of which the values are fixed by the three corresponding interfacial free energies, f_{GB}, f_{S1}, and f_{S2} [Fig. 5(a)]. This should result in a typical shape with a groove and a ridge on either side [1]. Because of surface diffusion, this entire shape should grow in size. In this way, surface diffusion can increase the roughness. Note that high GB energies imply small angles α_{GB} and, therefore, steep slopes at the groove.

Figure 5(b) sketches how we expect this GB grooving process to proceed on a polycrystalline film, in the absence of GB motion. Through surface diffusion, a local equilibrium situation is reached when the GBs are connected with one another by convex surfaces, each with constant curvature [24]. We have never observed configurations such as those in the first two panels of Fig. 5(b) at any stage of the evolution of the films. As in Fig. 4, all profiles look very similar to the third panel of Fig. 5(b). From this observation we conclude that over the entire range of conditions (temperatures) surface diffusion has been sufficiently fast to keep the surface shape in or close to equilibrium with the evolving GB configuration. Further evidence for this conclusion comes from STM movies [18], which show that each change in roughness takes place almost completely *during* a change in GB configuration. Only very modest shape relaxations are seen after that (see also Fig. 2), e.g., when the film is kept at constant temperature for some time. This implicitly demonstrates that even the special diffusion barriers at steps [25–28], which might cause an additional contribution to the roughness in the early stages of the film evolution, do not prevent the surface to "adiabatically" follow the evolving GB configuration.

We now use the above arguments to explain the observed roughness evolution of Fig. 3(b). In the freshly deposited film the relative grain orientations are often quite unfavorable, so that the average GB energy is high. This makes the average GB angle α_{GB} small, which, in turn, results in tall structures that make the film rough [Fig. 5(c)]. If the film is heated up, the GBs become mobile and quickly reorient themselves in lower-energy configurations (cusps in the energy versus orientation diagram of the GBs). In this way the average GB energy is lowered and the average α_{GB} increases, which explains the initial drop in roughness [Fig. 5(c)], as observed in Fig. 3(b) up to an average grain size of $\sim$100 nm. Next to this reorientation, the GBs also migrate. This GB migration leads to a gradual coarsening of the GB network. This in itself has no affect on the average α_{GB} and on the

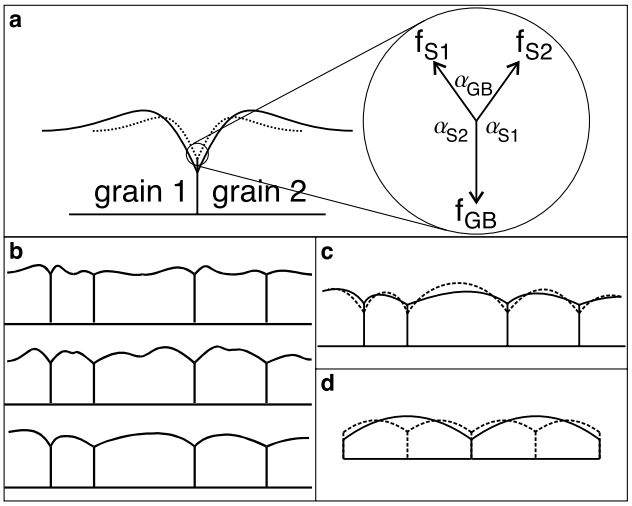

FIG. 5. (a) The equilibrium angles at a triple line are determined by the interface free energies. Large values of f_{GB} correspond to small angles α_{GB}. The dotted surface contour represents an earlier stage of the grooving. (b) Sketch of the grooving of a polycrystalline surface for a stationary grain size configuration. (c),(d) Film evolution resulting from changes in the GB configuration; the dotted lines represent the initial situation (c) a lower average GB energy results in a smoother surface, while (d) shows an increase in the average grain size results in a rougher surface.

average grain shape, since the average GB energy remains the same. But as the grain diameter increases, so does the height variation on each grain [Fig. 5(d)]. In the later stages of the film evolution, this leads to a gradual increase in film roughness, proportional to the average grain diameter, as expected for a self-similar scaling behavior, and observed for average grain sizes above 175 nm [Fig. 3(b)]. In the intermediate size regime, from 100 to 175 nm, the competing effects of the two processes, namely, GB reconfiguration and grain growth, cancel, and there is no net variation in film roughness.

The maximum average grain size, obtained after prolonged annealing at the highest temperature of 748 K, amounted to $\sim$300 nm, which is an order of magnitude larger than the film thickness. This is probably the maximum average grain size that can be reached for such a thin film, in accordance with theoretical predictions that are based on film-surface and film-substrate interface energies, in combination with the condition of mass conservation [similar to Fig. 5(d)] [29,30].

In summary, we have used STM to observe the irreversible evolution of a thin, polycrystalline metal film over a wide temperature range. Atomic step resolution enabled us to visualize grain boundaries and their motion. During the film evolution, the roughness was found to first decrease and later increase again. The decrease is caused by the initial rearrangement of the GBs, while the later increase is a natural consequence of the gradual coarsening of the grain boundary network. We expect similar evolution behavior for other metal films.

We acknowledge S. M. Yalisove for drawing our attention to polycrystalline metal films. This work is part of the research program of the Stichting voor Fundamenteel Onderzoek der Materie (FOM) and is financially supported by the Nederlandse Organisatie voor Wetenschappelijk Onderzoek (NWO).

[1] W.W. Mullins, J. Appl. Phys. **28**, 333 (1957).
[2] W.W. Mullins, Acta Metall. **6**, 414 (1958).
[3] L. Margulies *et al.*, Science **291**, 2392 (2001).
[4] H. van Swygenhoven, Science **296**, 66–67 (2002).
[5] C. E. Krill *et al.*, in *Developments in X-Ray Tomography III*, edited by U. Bonse, SPIE Proceedings Vol. 4503 (SPIE-International Society for Optical Engineering, Bellingham, WA, 2002), p. 205.
[6] B. C. Larson *et al.*, Nature (London) **415**, 887 (2002).
[7] M. Furtkamp *et al.*, Acta Mater. **46**, 4103 (1998).
[8] D. A. Molodov *et al.*, Acta Mater. **46**, 553 (1998), and references therein.
[9] U. Czubayko *et al.*, Acta Mater. **46**, 5863 (1998).
[10] C. S. Nichols *et al.*, Acta Metall. Mater. **41**, 1861 (1993).
[11] C.V. Thompson *et al.*, J. Appl. Phys. **67**, 4099 (1990).
[12] R. Dannenberg *et al.*, Thin Solid Films **370**, 54 (2000).
[13] R. D. Doherty *et al.*, Mater. Sci. Eng., A **238**, 219 (1997).
[14] C.V. Thompson, Annu. Rev. Mater. Sci. **20**, 245 (1990).
[15] C.V. Thompson, Annu. Rev. Mater. Sci. **30**, 159 (2000).
[16] Total roughness $\leq$ 2 nm over a length scale of 400 mm. The supplier was Crystal GmbH, Berlin, Germany.
[17] M. S. Hoogeman *et al.*, Rev. Sci. Instrum. **69**, 2072 (1998).
[18] See EPAPS Document No. E-PRLTAO-91-049328 for STM movies. A direct link to this document may be found in the online article's HTML reference section. The document may also be reached via the EPAPS homepage (http://www.aip.org/pubservs/epaps.html) or from ftp.aip.org in the directory /epaps/. See the EPAPS homepage for more information.
[19] Y. Golan *et al.*, Surf. Sci. **264**, 312 (1992).
[20] J. A. Floro *et al.*, MRS Bull. **27**, 19 (2002).
[21] D. Porath *et al.*, J. Vac. Sci. Technol. B **14**, 30 (1996).
[22] N. Mancini and E. Rimini, Surf. Sci. **22**, 357 (1970).
[23] T. S. Lin and Y.W. Chung, Surf. Sci. **207**, 539 (1989).
[24] The equilibrium condition of the film requires the absence of a net atom current, which is only realized if the two-dimensional curvature is constant everywhere at the film surface. The equilibrium condition at the GB grooves introduces extra energy terms that may lead to differences in the curvatures of different grains.
[25] G. Ehrlich and F. G. Hudda, J. Chem. Phys. **44**, 1039 (1966).
[26] R. Schwoebel, J. Appl. Phys. **37**, 3682 (1966).
[27] R. Schwoebel, J. Appl. Phys. **40**, 614 (1969).
[28] M. Kalff *et al.*, Surf. Sci. **426**, L447 (1999).
[29] T. P. Nolan *et al.*, J. Appl. Phys. **71**, 720 (1992).
[30] Z. G. Xiao *et al.*, MRS Proc. **202**, 101 (1991).